Sub-Arcsecond Morphology of Planetary Nebulae

L. F. Miranda[A,B,D], *G. Ramos-Larios*[A,C]*, and M. A. Guerrero*[A]

[A] Instituto de Astrofísica de Andalucía – CSIC, Granada, Spain
[B] Facultade de Ciencias, Universidade de Vigo, Vigo, Spain
[C] Instituto de Astronomía y Meteorología, Guadalajara (Mexico)
[D] Corresponding author. Email: lfm@iaa.es

Abstract: Planetary nebulae (PNe) can be roughly categorized into several broad morphological classes. The high quality images of PNe acquired in recent years, however, have revealed a wealth of fine structures that preclude simplistic models for their formation. Here we present narrow-band, sub-arcsecond images of a sample of relatively large PNe that illustrate the complexity and variety of small-scale structures. This is especially true for bipolar PNe, for which the images reveal multi-polar ejections and, in some cases, suggest turbulent gas motions. Our images also reveal the presence or signs of jet-like outflows in several objects in which this kind of component has not been previously reported.

Keywords: circumstellar matter — ISM: jets and outflows — planetary nebulae

1 Introduction

Planetary nebulae (PNe) consist of material ejected from the Asymptotic Giant Branch (AGB) progenitor, which is photoionized by the hot central star and swept up by the fast stellar wind (Kwok, Purton & Fitzgerald 1978). The morphology of PNe has attracted the attention of many observers because it is related to and contains information about the processes of mass ejection involved in their formation. A number of investigations have been devoted to the morphological classification of PNe (Balick 1987; Schwarz, Corradi & Melnick 1992; Stanghellini, Corradi & Schwarz 1993; Manchado et al. 1996). In general, three broad morphological classes have been considered: round (or circular), elliptical and bipolar. The formation of the three classes was explained within the Generalized Interacting Stellar Winds (GISW) Model (Balick 1987) assuming an azimuthal dependence of the density in the slow wind, having its maximum at the equatorial plane. Bipolar and elliptical PNe would present 'high' and 'intermediate' density contrasts, while round PNe would present a homogeneous slow wind. Numerical simulations have shown that the three main morphological classes can be reproduced under this hypothesis (e.g. Frank et al. 1993).

The detection of collimated outflows in PNe (e.g. Gieseking, Becker & Solf 1985; Miranda & Solf 1992) poses a serious difficulty to the GISW model because this model is unable to explain the presence of highly collimated ejections. Moreover, no collimating agent was foreseen in these evolutionary phases, which could cause high collimation. In addition, the collimated ejections in most PNe present different orientations with respect to the central star suggesting that the collimated agent can precess or wobble (Miranda & Solf 1992; Miranda, Guerrero & Torrelles 1999; Guerrero et al. 2008).

More recently, high-resolution images obtained with the *Hubble Space Telescope HST* have shown that PNe are highly complex objects and that simplistic models are unable to account for the large variety of structures and microstructures observed in these objects. In particular, the signature of collimated outflows appears in a very large fraction of PNe (e.g. Sahai & Trauger 1998). Many PNe show multiple bipolar ejections with different geometries that require episodic ejections (e.g. Guerrero, Chu & Miranda 2004). These observations have led to suggest that collimated outflows are the basic mechanism that shapes PNe (Sahai & Trauger 1998). Nevertheless, other physical phenomena should be also present in PN formation as wind interaction, magnetic fields and/or the binary nature of the central star (see Balick & Frank 2002). Although a large number of PNe have already been imaged (Balick 1987; Schwarz et al. 1992; Manchado et al. 1996; Sahai & Trauger 1998), in some cases the images lack spatial resolution and/or quality to enable a proper identification of the morphological components. In fact, images at higher resolution and/or deeper than previous ones continue discovering new structures, even in well observed PNe, which result to be key for a proper interpretation of their formation (e.g. Maestro, Guerrero & Miranda 2004; Miranda et al. 2006). These results and the complexity of PNe clearly justify the imaging of PNe whose images are of insufficient quality.

In this paper, we present narrow-band images of a sample of relatively large PNe, including elliptical and bipolar PNe. The images have been taken under particularly good seeing conditions and reveal novel details in the objects.

2 Sample Selection and Observations

The observed PNe were selected from the Manchado et al. (1996) catalog among those with no independent Hα and [NII] images and/or with low resolution images due to poor seeing conditions. Images isolating the Hα and [NII] lines are crucial because these two emission lines may trace very different regions of the nebulae; in particular, collimated outflows and microstructures can be better recognized and studied in [NII]. In addition, good seeing conditions allow us a detailed morphological study of the structures present in a PN. We have added IC 5217 and NGC 6778 to this sample in order to study at high spatial resolution the structures identified by Miranda et al. (2006) and Maestro et al. (2004), respectively.

Direct images were obtained on 2006 June and 2008 September using ALFOSC at the 2.56 m Nordic Optical Telescope on Roque de los Muchachos Observatory (La Palma, Spain). A 2K × 2K E2V CCD with plate scale of $0.19''$ pixel^{-1} was used as detector. We used three narrow-band filters that isolate the light of Hα ($\Delta\lambda = 9$ Å), [NII]$\lambda 6584$ (hereafter [NII]) ($\Delta\lambda = 9$ Å) and [OIII]$\lambda 5007$ (hereafter [OIII]) ($\Delta\lambda = 30$ Å). Exposure time per filter was 900 s or 1800 s. The seeing during the observations was between $0.5''$ and $0.9''$. The images were reduced using standard IRAF routines.

3 Results and Discussion

In the following we will discuss the images of the objects observed. In some cases, we have grouped together some objects because of their morphological similarities.

3.1 IC 351 and Vy 1-1

In the Manchado et al. (1996) catalog, IC 351 is classified as an elliptical PNe with internal structures while Vy 1-1 is classified as an elliptical multiple-shell PN. The two objects are not included in the lists of PNe with low-ionization structures, knots or jets by Goncalves, Corradi & Mampaso (2001).

Figures 1 and 2 show our images of IC 351 and Vy 1-1, respectively. The two PNe present noticeable morphological similarities, including low-ionization polar structures which are identified in these images for the first time.

IC 351 is a high-excitation PN consisting of an inner elliptical shell oriented along PA ∼355° surrounded by an outer round attached shell. The central star is detected in the [NII] and [OIII] filters. The [NII] image shows two collimated structures emanating from bright polar caps of the inner elliptical shell that extend ∼$3''$ and end in bright knots. The Hα and [OIII] images also show hints of these structures but they are relatively much fainter, implying low-excitation.

Vy 1-1 (Figure 2) shows an inner elliptical shell oriented at PA ∼70°, and an outer round attached shell. Although no [OIII] image has been obtained for Vy 1-1, the faint emission in [NII] and the bright emission in [OIII] (see Manchado et al. 1996) indicate that both shells are of high-excitation. The polar regions of the inner shell are
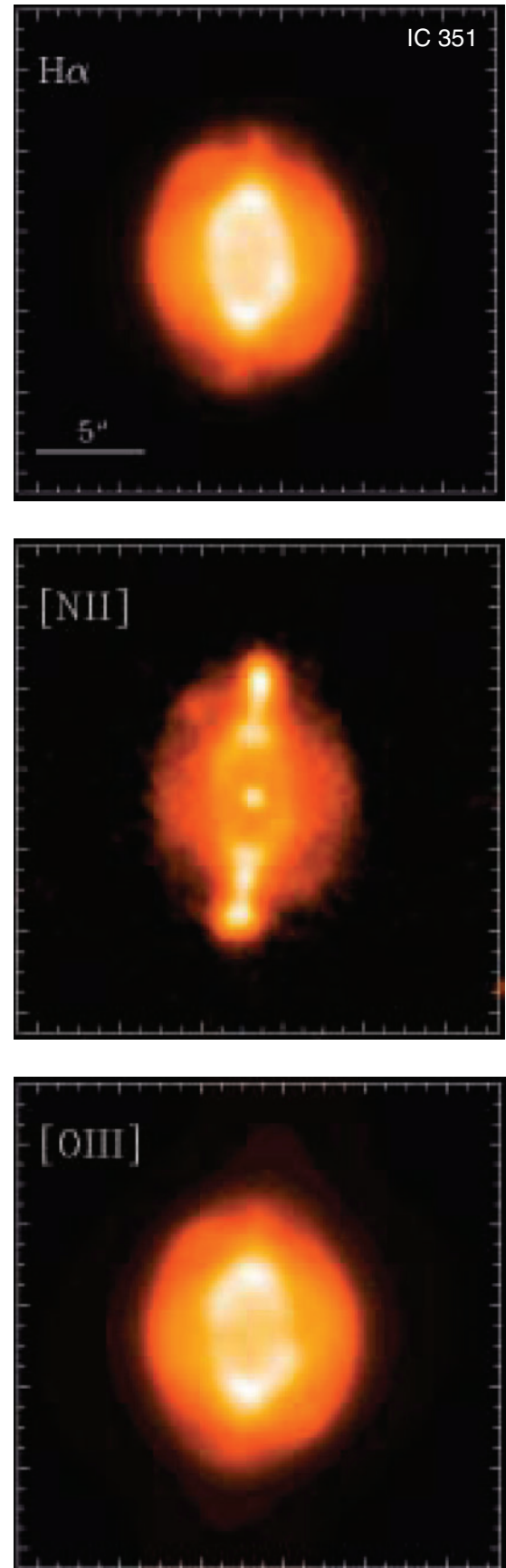

Figure 1 Hα, [OIII] and [NII] images of IC 351. North is up, east to the left. The images are displayed in a logarithmic scale. White represents high values of the intensity.
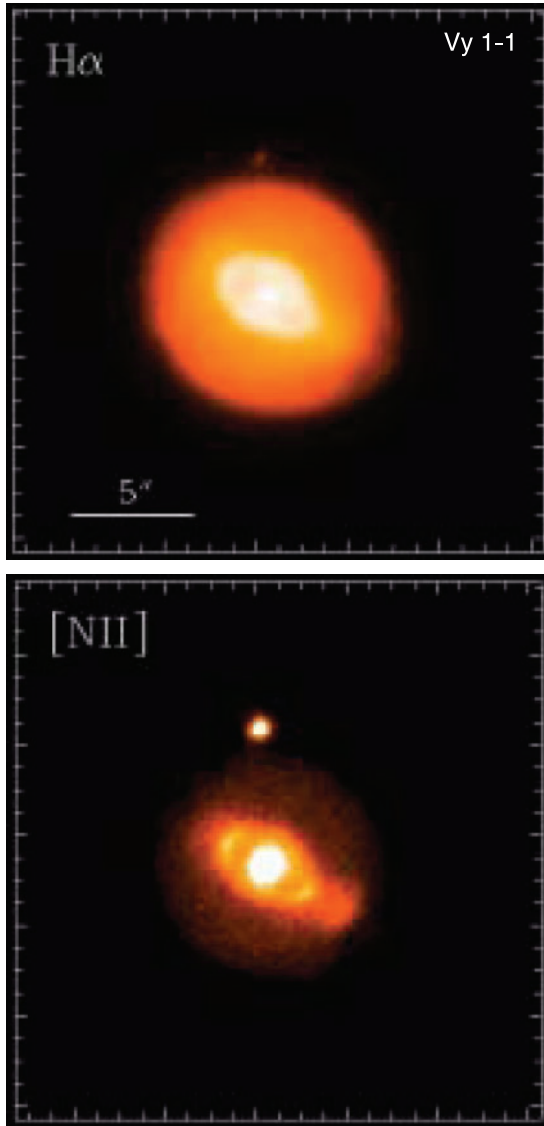
Figure 2 Hα and [NII] images of Vy 1-1. North is up, east to the left. The images are displayed in a logarithmic scale. White represents high values of the intensity.

Figure 3 (Top) Colour composite picture of NGC 6778 (green = Hα, blue = [OIII] and red = [NII]). The image is displayed in a logarithmic scale. (Bottom) Unsharp masking [NII] image. The image is displayed in a linear scale. North is up, east to the left in the images.

particularly bright in [NII]. Two polar knots are observed outside but connected to the elliptical inner shell in the [NII] image; they are not recognizable in the Hα image. The south-western knot is brighter than the north-eastern one.

IC 351 and Vy 1-1 closely resemble NGC 6826 and NGC 7009 (Balick et al. 1998). Although the radial velocities of the polar structures in IC 351 and Vy 1-1 have not been measured, it is probable that they represent FLIERs as in the case of NGC 6826 and NGC 7009. The morphological resemblances suggest similar formation processes in the four PNe.

3.2 NGC 6778

NGC 6778 is a PN that contains two bipolar jet systems oriented at different directions and moving at 100–200 km s^{-1} (Maestro et al. 2004). Figure 3 shows a colour
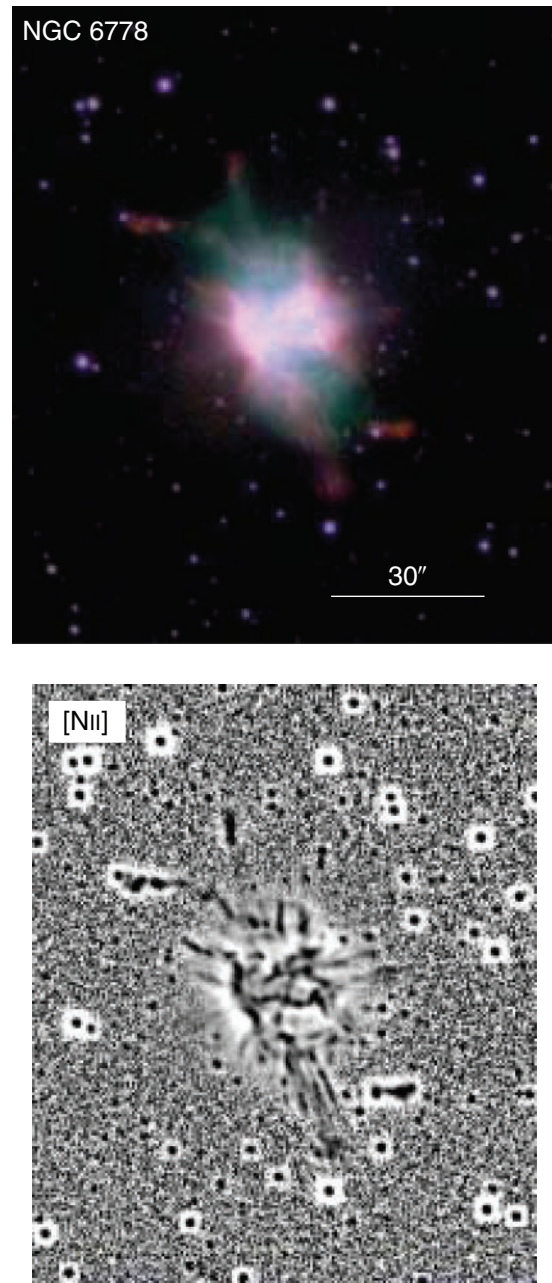
composite picture of NGC 6778 constructed with the Hα, [OIII] and [NII] images. The high resolution of the new images allow us a detailed description of the nebulae. The appearance of NGC 6778 is that of a bipolar nebula with its major axis along PA $\simeq 15°$. The nebula does not display the characteristic waist of butterfly PNe, but the region along its minor axis is defined by a fragmented structure that is particularly bright in [NII]. In the high-excitation [OIII] emission, the nebula appears elliptical rather than bipolar. The images reveal details of the bipolar jets. In particular, the jet oriented at PA $\simeq 195°$ consists

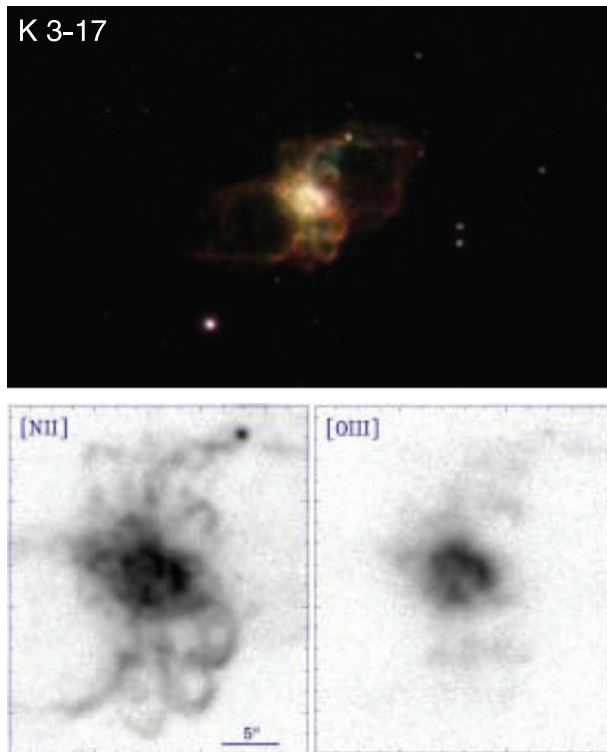**Figure 4** (Top) Colour composite picture of K 3-17 (green = Hα, blue = [OIII] and red = [NII]). (Bottom) Enlargement of the bright central region in the [NII] and [OIII] images. The images are displayed in a logarithmic scale. North is up, east to the left in the images. The spatial scale is indicated in the [NII] image.

Figure 5 (Top) Hα image of IC 5217 showing the whole bipolar structure and the point-symmetric features. North is up, east to the left. (Bottom) Images of the equatorial regions in several filters (upper left). The central star is observed in the [SII] filter. The images are displayed in a logarithmic scale.

of at least four filaments emanating from a bright knot. In addition, the nebula presents many low-excitation knots with a cometary appearance, embedded in high-excitation material. These knots are more clearly observed in the unsharp masking [NII] image also shown in Figure 3. This image further strengthens the complexity of the nebula. We found interesing similarities between NGC 6778 and Sh 2-71 (Bohigas 2001; Miranda et al. 2005) as both PNe exhibit extremely knotty and filamentary morphologies that suggests that the previously existing structures have been fragmented and probably swept up by the fast stellar wind.

3.3 K 3-17

K 3-17 presents a bipolar morphology in the Manchado et al. (1996) catalog consisting of a bright compact core and two faint bipolar lobes in the Hα+[NII] image. In the [OIII] image only the bright compact core was detected. Our new, higher resolution images reveal that K 3-17 is a complex PN with a wealth of structures. A colour composite picture is shown in Figure 4 along with [NII] and [OIII] images of the bright core. In the new images, the bipolar lobes present a spindle-like shape and are dominated by [NII] emission. The core is resolved into a series of bubbles oriented mainly perpendicular to the bipolar lobes, although small bubbles oriented along the bipolar axis are also observed. No ring-like or toroidal structure can be
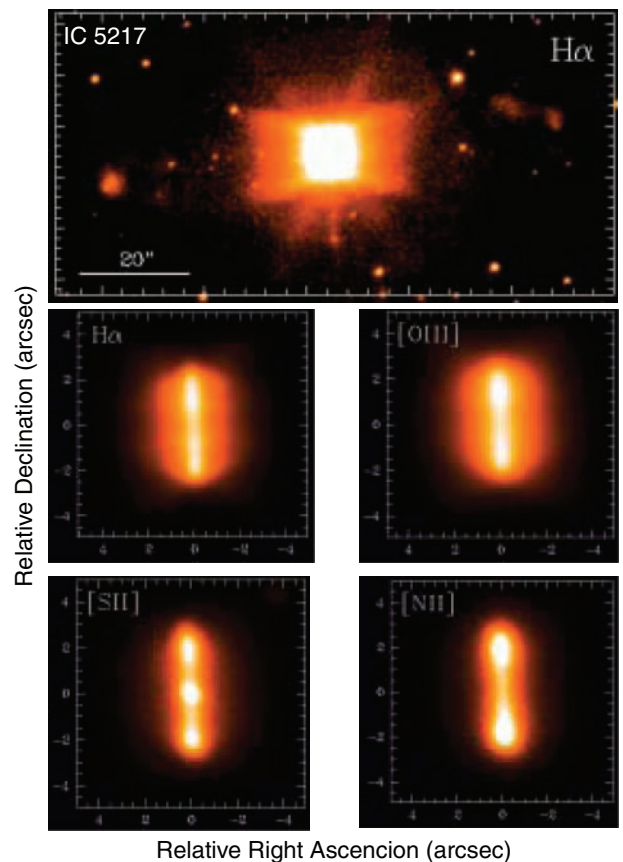
identified in the center but bright knots without a particular orientation. Most of the structures are of low-excitation while high-excitation is only observed at the central knots and in the regions of the lobes near the center.

The spindle-like morphology of the lobes suggests the action of collimated outflows in their formation. A similar morphology is observed in Hu 2-1 in which the distorsions of the lobes can be attributed due to the action of a bipolar collimated outflows (Miranda et al. 2001). As for the origin of the equatorial bubbles in K 3-17, it could be possible that the stellar wind is protruding through or breaking an original equatorial structure. Alternatively, the bubbles may represent collimated outflows along different directions. In this case, the orientation of the collimation axis should have changed drastically by ≃90°. Large differences in the orientation of multipolar lobes are also found in other PNe, being Sh 2-71 an extreme case (Miranda et al. 2005), while the equatorial bubbles in K 3-17 are similar to these observed in *HST* images of Hb 5 (see Montez et al. 2009).

4 IC 5217 and KjPn 6

IC 5217 is an edge-on bipolar PN with polar point-symmetric features, a large axial ratio and a narrow waist that contains a very thin, bright equatorial ring (Miranda et al. 2006).

Figure 5 presents a new Hα image and images of the ring in several emission lines. The large scale Hα image is similar to that presented by Miranda et al. (2006). In particular, the point-symmetric structures at large distances from the center are observed in this image as well as the bipolar lobes emanating from the nebular central regions that seem to be connected with the point-symmetric features. The higher resolution of the new images and the observations in several emission line filters allow us to analyze the bright equatorial ring in great detail. Four local maxima along the ring are distinguished in the Hα image in agreement with the radio continuum morphology at 3.6 cm (see Miranda et al. 2006). In the rest of the emission lines, a clear ionization gradient is observed with the radius of the ring in [OIII] being smaller than in [NII] and [SII]. We also note that the central star is detected in the [SII] image at the center of the ring. It is worth noting that, if only a short exposure image would have been acquired, IC 5217 would be described as a highly collimated bipolar jet emanating from the central star. This is not the case as high-resolution, long-slit spectroscopy demonstrates that the bright structure is an edge-on ring (Miranda et al. 2006).

KjPn 6 presents a peculiar, almost triangular shape in the Hα+[NII] image and extremely faint emission in the [OIII] image (Manchado et al. 1996). The new images of KjPn 6 are shown in Figure 6. The structure in Hα and [OIII] resembles an elliptical PN with the major axis near the north-south direction, while in [NII] the nebula appears more squarish. Faint details are observed in the inner regions, which are particularly bright in [NII] and Hα but absent in [OIII]. The morphology of KjPn 6 is very similar to this observed in the inner regions of IC 5217 (Figure 5), which have been identified with an edge-on ring. These similarities lead us to suggest that KjPn 6 may be a bipolar PN with bipolar much fainter than its equatorial regions. Therefore, IC 5217 and KjPn 6 are probably related to ring-like PNe that are characterized by the presence of a bright ring accompanied by faint bipolar lobes, although these are not always detected (e.g. Bond, Pollacco & Webbink 2003). Interesting similarites are found with the edge-on ring-like PNe Me 1-1 (Pereira et al. 2008) and IC 2149 (Vázquez et al. 1999).

5 Bipolar Planetary Nebulae

Figure 7 shows colour composite pictures of six bipolar PNe. The new images are deeper and of higher quality than these published elsewhere. BV 1 is an edge-on bipolar with a bright ring and extremely faint bipolar lobes (Kaler et al. 1988). HaTr 10, M 4-17, and K 3-46 are likely similar to BV 1, the main difference being the orientation of the polar axis with respect to the observer and/or the evolutionary stage. The case of NGC 650 could be different as this PN is observed almost edge-on, as is the case of BV 1, but the equatorial region is thick and there is not a large intensity contrast between this equatorial region and the bipolar lobes. In addition, NGC 650 shows bubbles and microstructures that suggest the presence of
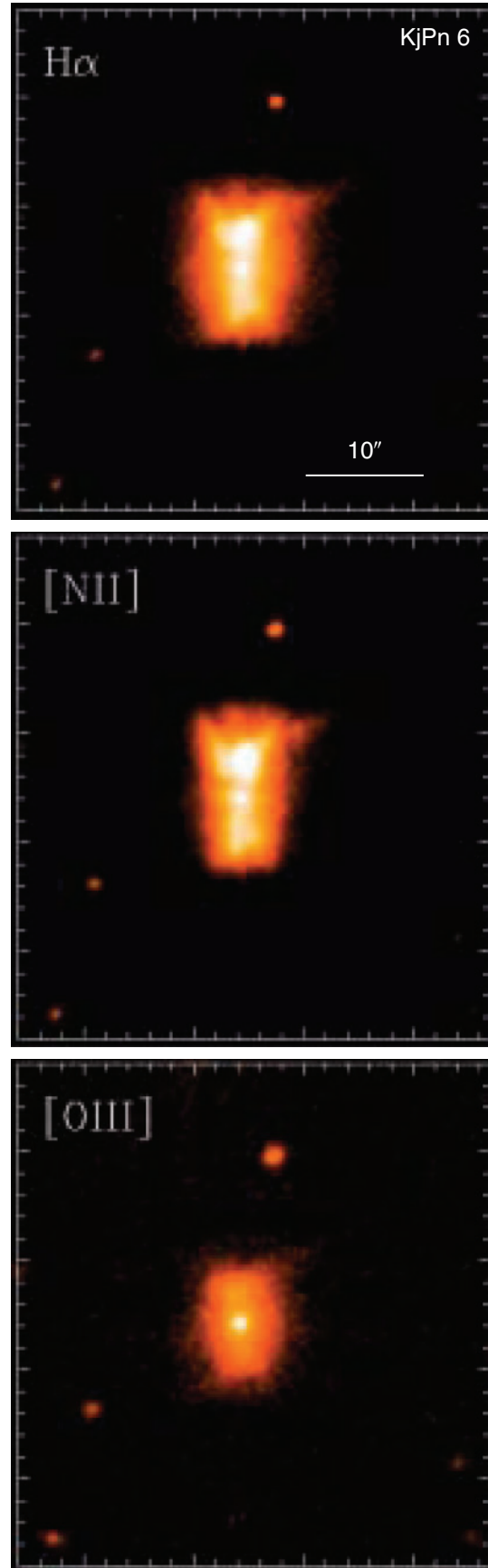

Figure 6 Hα, [NII] and [OIII] images of KjPn 6. The images are displayed in a logarithmic scale. North is up, east to the left in each image.
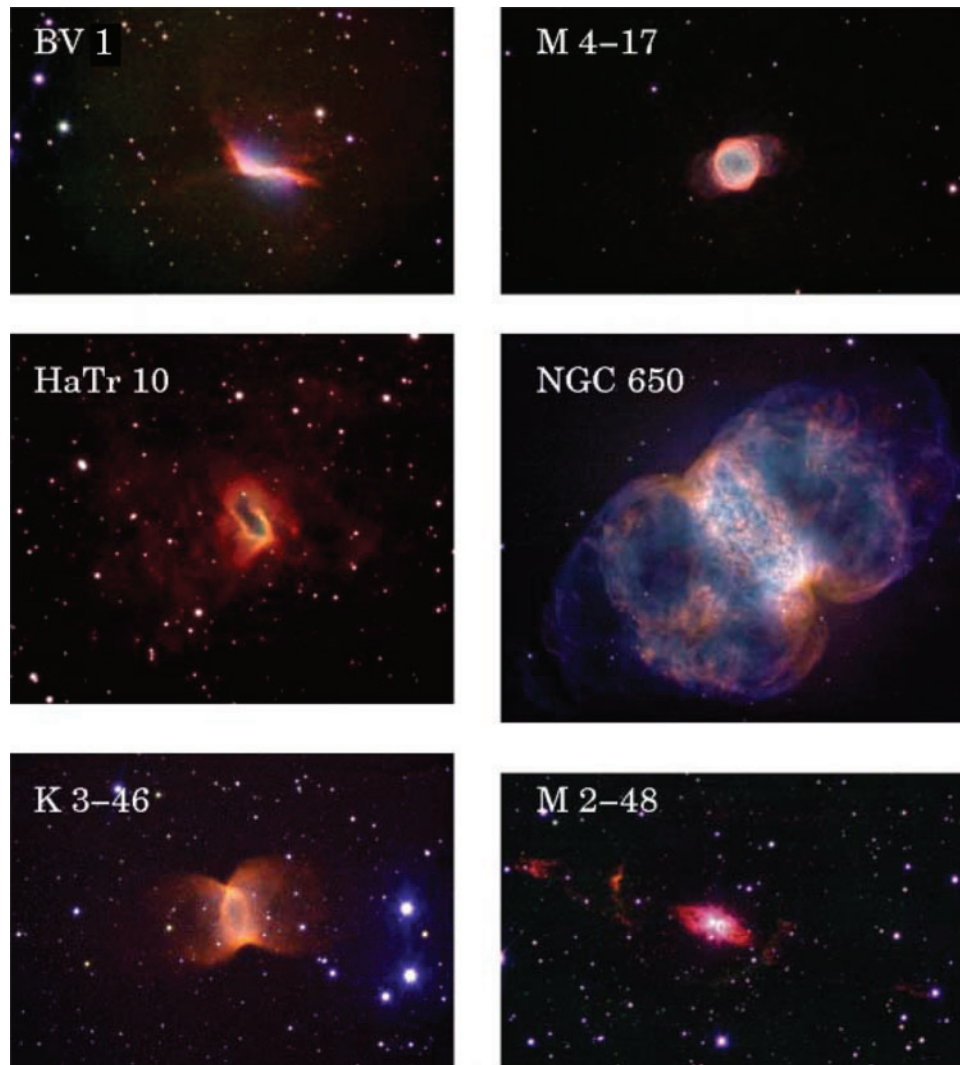
Figure 7   Colour composite pictures of BV 1 (field of view [fov] $\simeq 285'' \times 155''$), M 4-17 (fov $\simeq 255'' \times 130''$), HaTr 10 (fov $\simeq 170'' \times 140''$), NGC 650 (fov $\simeq 130'' \times 105''$), K 3-46 (fov $\simeq 215'' \times 150''$) and M 2-48 (fov $\simeq 245'' \times 155''$). In all cases the colour code is green = Hα, blue = [O III] and red = [N II]. The images are displayed in a logarithmic scale. North is up, east to the left in each image.

focused (collimated) outflows. M 2-48 is a bipolar PN with multiple structures and high velocity collimated outflows (Vázquez et al. 2000; López-Martín et al. 2002). Our high resolution image (Figure 7) shows in great detail the structures previously detected. A dark lane, rather than a bright equatorial torus or ring, separates the bipolar lobes. Elongated protrusions are observed along the minor axis of the nebula, although their orientation is different from this of the bipolar lobes and collimated outflows. A series of knots encircle the bipolar lobes tracing an apparent circular shell. This shell is brighter at four regions along the main symmetry axis and its center does not coincide with the nebular core. The distant outflows discovered by Vázquez et al. (2000) appear as knotty structures, particularly the north-eastern one. Its south-western counterpart is clearly detected in the new images, while only hints of it were found by Vázquez et al. (2000). M 2-48 presents noticeable differences when compared to the other bipolar PNe in Figure 7. On the other hand, the presence of distant

outflows in M 2-48 resembles the situation observed in IC 5217 (see above).

6 Final Remarks

Images obtained at sub-arcsec resolution ($0.5''$–$0.9''$) have revealed new morphological details in selected PNe. In IC 351 and Vy 1-1, low-excitation, jet-like features have been detected for the first time. The morphology of these two objects is very similar to this of well studied PNe like NGC 6826 and NGC 7009, strongly suggesting that the same processes have operated in the formation of these objects. In NGC 6778 and K 3-17 we found very complex structures. NGC 6778 consists of a large number of cometary knots and filaments with two systems of collimated outflows. K 3-17 presents equatorial bubbles oriented at different directions. Evidence for collimated outflows in K 3-17 is provided by the spindle-like bipolar lobes. IC 5217 and KjPn 6 are bipolar PNe consisting in a bright edge-on equatorial ring and faint bipolar lobes.

A comparison of the bipolar PNe in the sample suggests that the formation processes of NGC 6778, K 3-17 and M 2-48, implying the action of collimated outflows, may differ from this of NGC 650, K 3-46 and BV 1 which fit the expectations of the GISW model.

Acknowledgments

References

Balick, B., 1987, AJ, 94, 671
Balick, B. et al., 1998, AJ, 116, 360
Balick, B. & Frank, A., 2002, ARA&A, 40, 439
Bohigas, J., 2001, RMxAA, 37, 237
Bond, H. E., Pollacco, D. L. & Webbink, R. F., 2003, AJ, 125, 260
Frank, A., Balick, B., Icke, V. & Mellema, G., 1993, ApJ, 404, L25
Gieseking, F., Becker, I. & Solf, J., 1985, ApJ, 295, L17
Goncalves, D. R., Corradi, R. L. M. & Mampaso, A., 2001, ApJ, 547, 302
Guerrero, M. A., Chu, Y.-H. & Miranda, L. F., 2004, AJ, 128, 1694
Guerrero, M. A. et al., 2008, ApJ, 683, 272

Kaler, J. B., Chu, Y.-H. & Jacoby, G. H., 1988, AJ, 96, 1407
Kwok, S., Purton, C. R. & Fitzgerald, P. M., 1978, ApJ, 219, L125
López-Martín, L. et al., 2002, A&A, 388, 652
Maestro, V., Guerrero, M. A. & Miranda, L. F., 2004, ASPC, 313, 127
Manchado, A., Guerrero, M. A., Stanghellini, L. & Serra-Ricart, M., 1996, The IAC Morphological Catalog of Northern Galactic Planetary Nebulae (La Laguna: Instituto de Astrofísica de Canarias)
Miranda, L. F., Ayala, S., Vázquez, R. & Guillén, P. F., 2006, A&A, 456, 591
Miranda, L. F., Ayala, S., Ulla, A., Olguín, L. & Vázquez, R., 2005, in IAP Conference Proceedings, 804, Planetary Nebulae as Astronomical Tools, Eds. Szczerba, R., Stasińska, G. & Górny, S. K. (New York: IAP), 97
Miranda, L. F., Guerrero, M. A. & Torrelles, J. M., 1999, AJ, 117, 1421
Miranda, L. F. & Solf, J., 1992, A&A, 260, 397
Miranda, L. F., Torreles, J. M., Guerrero, M. A., Vázquez, R. & Gómez, Y., 2001, MNRAS, 321, 487
Montez, R., Kastner, J. H., Balick, B. & Frank, A., 2009, ApJ, 694, 1481
Pereira, C. B., Miranda, L. F., Smith, V. V. & Cunha, K., 2008, A&A, 477, 535
Sahai, R. & Trauger, J. T., 1998, AJ, 116, 1357
Schwarz, H. E., Corradi, R. L. M. & Melnick, J., 1992, A&AS, 96, 23
Stanghellini, L., Corradi, R. L. M. & Schwarz, H. E., 1993, A&A, 279, 521
Vázquez, R. et al., 2000, A&A, 357, 1031
Vázquez, R. et al., 2002, ApJ, 576, 860